# *The phase and pole structure of the N*(1535) and the issue of $\sigma_n/\sigma_p$ in $\eta N$ photoproduction within U$\chi$PT*


*Collaboration:*

*M. Döring (FZJ/UGA)*



- *M. Döring and K. Nakayama,*
  *EPJ**A43**, 83 (2010); PL**B683**, 145 (2010).*

# *Motivation:* *The nature of the N*(1535) resonance*

- UχPT: dynamically generated due to the strong coupling to the KΛ and KΣ channels dictated by SU(3) and the Kaon decay constant ($f_K \approx 113$ MeV).
- Meson Exchange Models: genuine (3-quark state) resonance. But, …

Schutz et al., PRC57,'98:
(πN,ηN,σN,πΔ, but no KΛ,KΣ)

cusp due to the ηN opening seems not to be present in the PWA of KA84 and SM95

favored genuine resonance over dynamical resonance

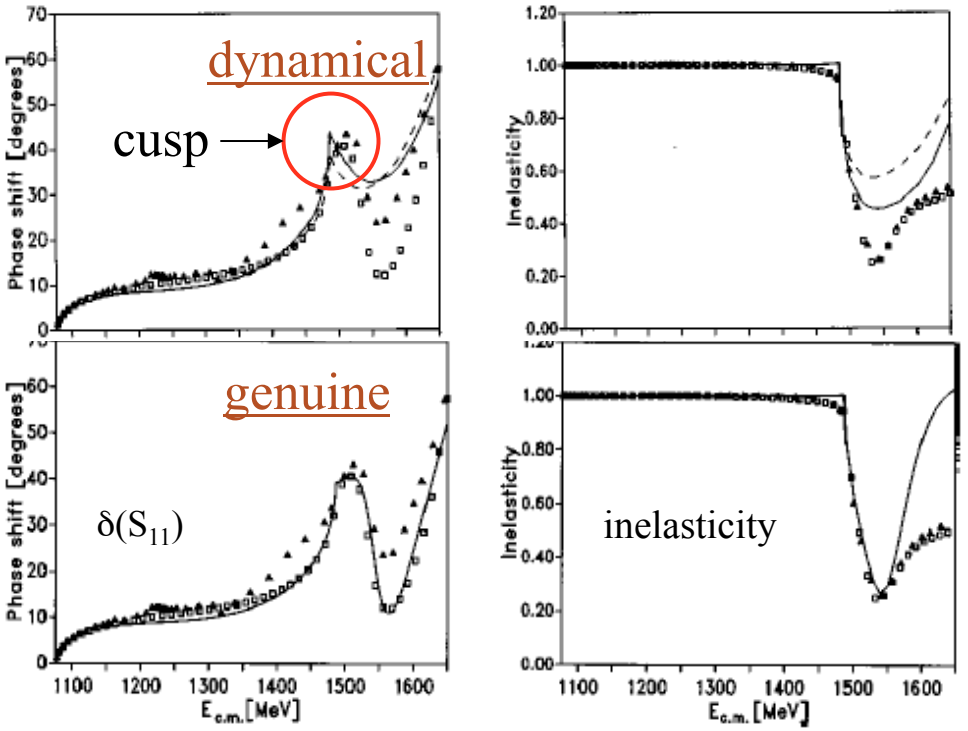


More recent models: multi-channel, but no KΛ and KΣ channels so far
(Jülich, EBAC) (remains to be seen once KΛ and KΣ channels are included)

# *Motivation:* *What has been done so far within the UχPT in the N*(1535) region:*

## Meson-Baryon amplitude:

$$T^{NP} = V^{NP} + V^{NP} G T^{NP}$$ ( matrix in channel space)

$V^{NP}$ = S-wave LO (Weinberg-Tomozawa)

- on-shell approximation ⇒ G→factorized propagator
  (for an off-shell treatment, see Borasoy et al., EPJA34,'07)
- non-relativistic approximations

## Photoproduction amplitude:

Attach photon everywhere possible to

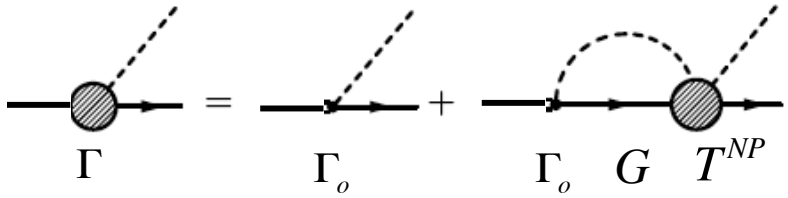


$$\Rightarrow M^{\mu} = V^{\mu} + V^{\mu} G T^{NP}$$ (vector in channel space) gauge invariant & unitary

$V^{\mu}$ = due to the interaction current a set of diagrams appears which consists of more than the usual u-, and t-channel (loop) diagrams.
(see, e.g., Borasoy et al., EPJA34,'07)

- non-relativistic approximations
- on-shell approximation of the photon vertex

# *Motivation:* *Existing calculations within the UχPT up to the N*(1535) region:*

- Many tests of hadronic models with an electromagnetic probe have been done at the cross section level only, mainly due to the scarcity of data.

- Radiative decay of the resonance has been also looked at, but its experimental extraction is tied to large uncertainties. (Döring et al., PRC74,'06; NPA786,'07)

- Helicity amplitudes $A^p_{1/2}$, $A^n_{1/2}$, and $S_{1/2}$ have been tested in rough agreement with the results extracted empirically. (Jido et al., PRC77,'07)

# *Results:* *Phase inconsistency of N*(1535) in πN→πN and γN→πN in the previous models (Inoue et al., PRC65,'02)*

$S_{11}$ ampl. in πN→πN

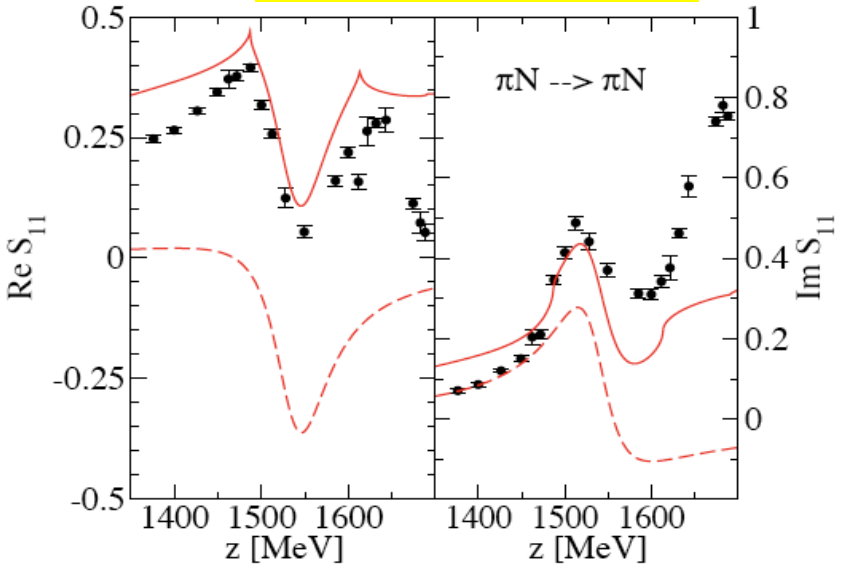


solid: original model (Inoue et al., PRC65,'02)
dashed: pole approx. of the above model
points: PWA (Arndt et al., PRC69,'04)

$E_{0+}$ in γN→πN

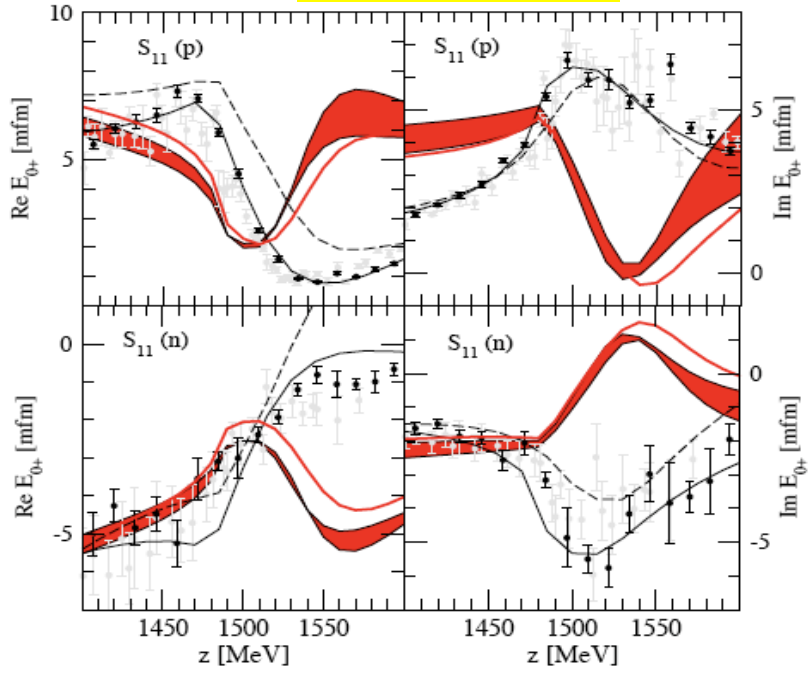


band: from full & simplified models (Inoue et al., PRC65,'02)
solid: from πN→πN refitted version of the above model
Points: black: SES-[FA07], (Arndt et al., PRC69,'04)
gray: SES-[FA06], (Arndt et al., PRC66,'02)
dashed: MAID2007, (Drechsel et al., EPJA34,'07)
solid: SAID [FA07], (Arndt et al., PRC69,'04)

# *Results:* *Phase inconsistency of N*(1535) in πN→πN and γN→πN in the previous models* *(Inoue et al., PRC65,'02)*

$S_{11}$ ampl. in πN→πN

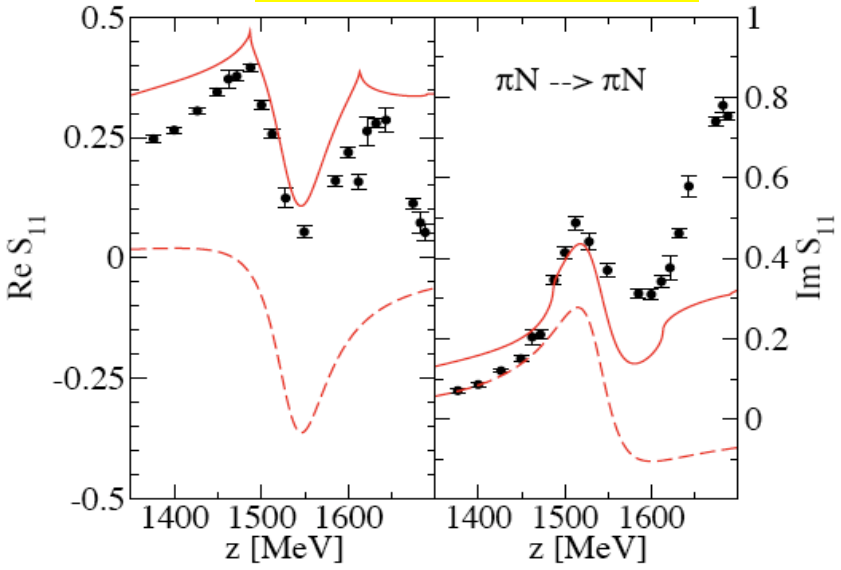


$E_{0+}$ in γN→πN

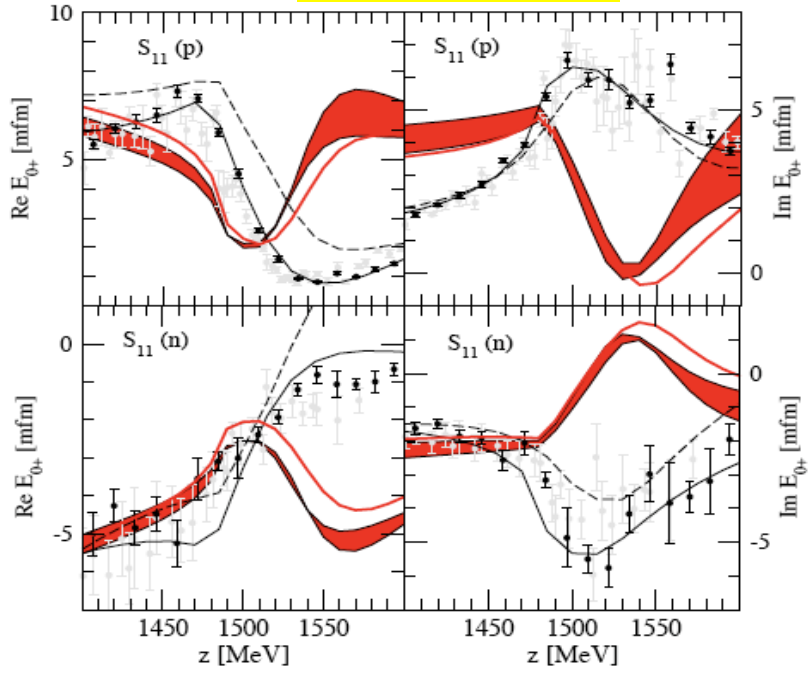


pole approximation:

$$T_{ij} = \frac{a_{-1}}{z - z_o} + a_o + a_1 + \mathrm{O}(z^2)$$

$$a_{-1} = g_i g_j$$

$$\varepsilon_\mu M^\mu = \frac{a^\gamma_{-1}}{z - z_o} + \ldots$$

$$a^\gamma_{-1} = g_\gamma g_j; \qquad g_\gamma = \Sigma(\tilde{\Gamma}^i g_i)$$

# *What we want to do*

- Access the relative phases of the N*(1535) in $\pi N \to \pi N$ and $\gamma N \to \pi N$ via the phase-shifts and $E_{0+}$ multipoles, where the PWA exist (Arndt et al., PRC66,'02; see also Drechsel et al., EPJA34,'07)

- Include the important resonance interference effects (see, e.g., Döring et al., NPA829,'07) with the nearby N*(1650) since this resonance is not included in the previous approaches.

# *Our Model:* *Meson-Baryon amplitude with genuine resonance*

$$T = V + VGT$$ (matrix in channel space: πN, ηN, KΛ, KΣ)

$$V = V^{P} + V^{NP} \rightarrow T = T^{P} + T^{NP}$$

$\Gamma_o g_o \Gamma_o^{T}$ (genuine resonance)

Weinberg-Tomozawa
- non-relativistic
- on-shell factorization

$$\begin{cases} T^{NP} = V^{NP} + V^{NP} G T^{NP} \\ T^{P} = \Gamma\, g \Gamma^{T}, \end{cases} \qquad \begin{cases} \Gamma = (1 + T^{NP} G)\Gamma_o \\ g = (g_o^{-1} - \Sigma) \end{cases}$$

$\Gamma_o G \Gamma$ (self-energy matrix)

$$\begin{cases} \Gamma_o = \dfrac{k}{f_\pi}[g_8 c_s + g_{8'} c_a + g_{\overline{10}} c_d + g_{27} c_{27}] \\ g_o^{-1} = z - m_o \end{cases}$$ (vector in channel space)

# *Our Model:* *Photoproduction amplitude based on the field theoretical approach of Haberzettl (PRC56,'97)*

The full field theoretical approach of Haberzettl results in highly non-linear amplitude and impractical to be implemented in an actual calculation. More recently, Haberzettl et al. [PRC74,'06] have derived an amplitude where the complicated part of the interaction current is approximated by generalized contact currents. The resulting amplitude is gauge invariant and unitary. This approach can be adapted to the present coupled-channel approach. The result is

$$M^{\mu} = M^{\mu}_{s} + M^{\mu}_{u} + M^{\mu}_{t} + M^{\mu}_{c} + T^{\mu} + [M^{\mu}_{tT} + M^{\mu}_{uT} + T^{\mu}]\tilde{G}T^{NP}$$

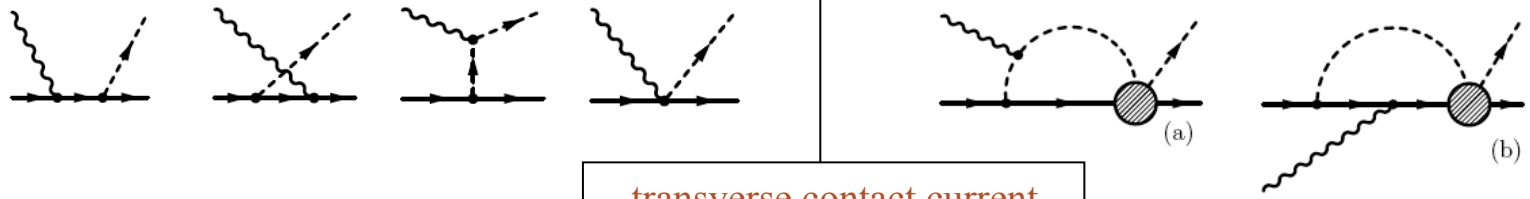


transverse contact current
(unconstrained by gauge invariance)
set to zero

$$+[M^{\mu}_{s}]_{N^*}$$

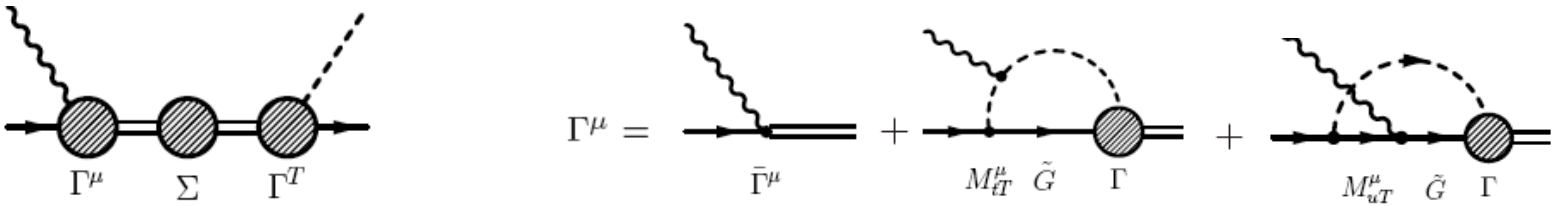

# *Results:* *Low energy πN→πN and γN→πN results in the present model (no resonances)*

$S_{11}$ & $S_{31}$ ampl. in πN→πN

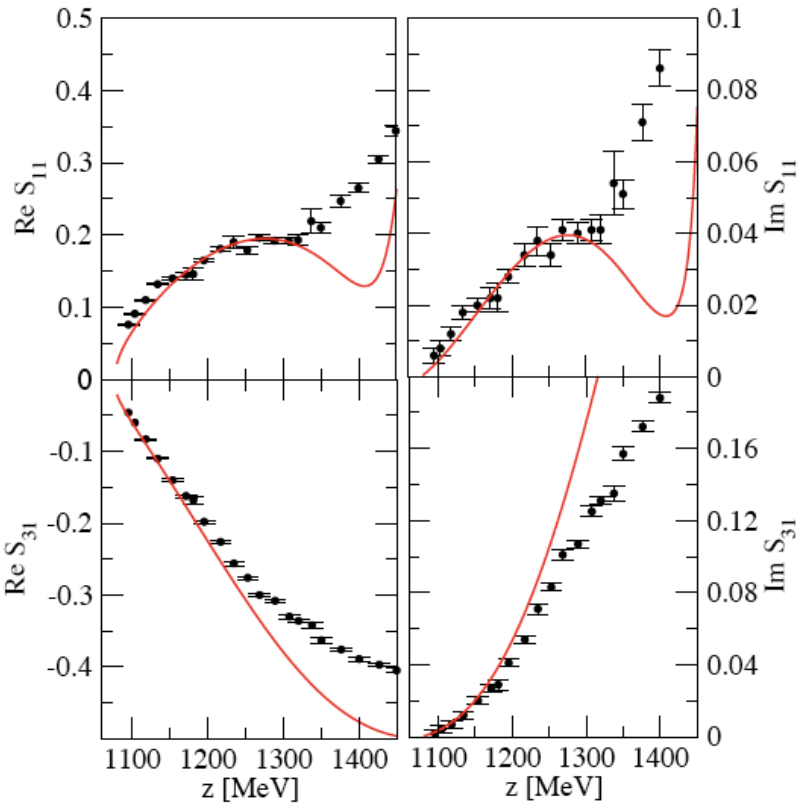


FIG. 9: (Fit 1) Low energy pion scattering. Analysis without resonances. Data from partial wave analyses as in Fig. 7.

$E_{0+}$ in γN→πN

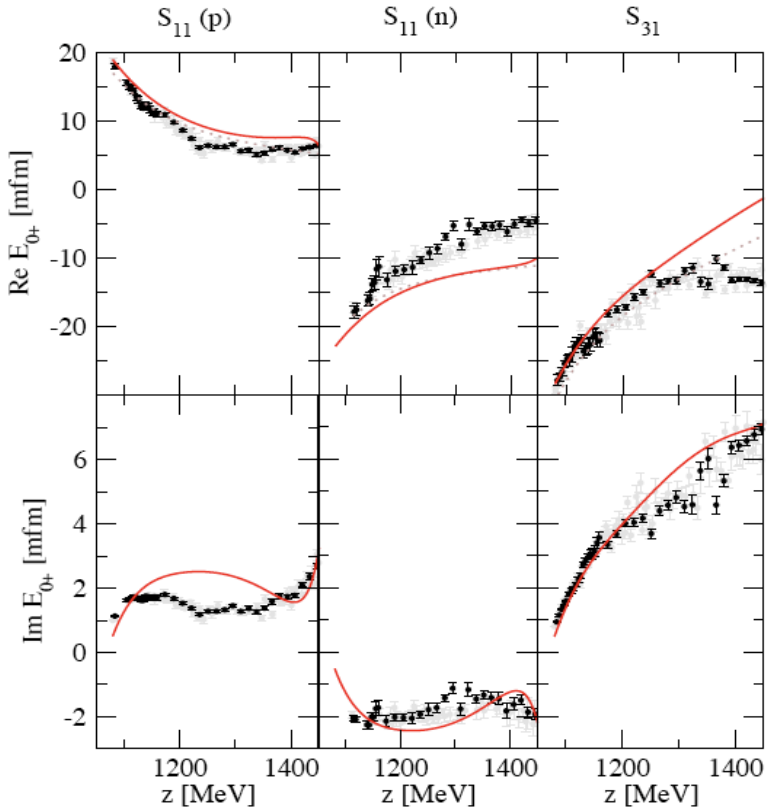


FIG. 10: (Fit 1) Low energy pion photoproduction. Analysis without resonances. Data from partial wave analyses as in Fig. 6.

# *Results:* *Threshold $\gamma p \to \pi^0 p$ (cont.')*

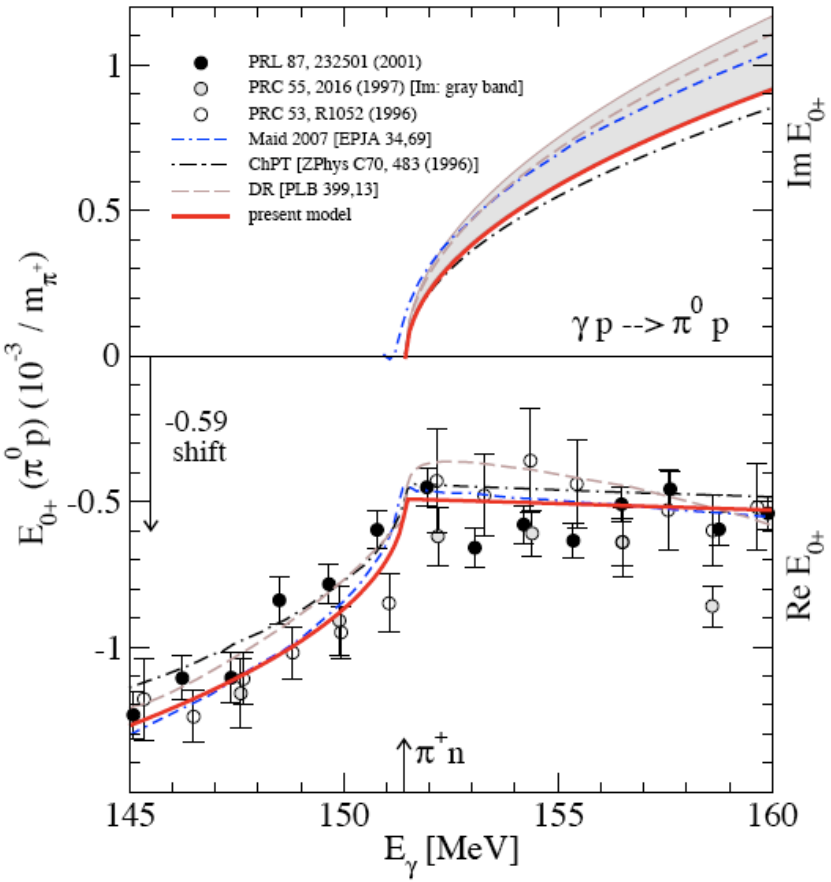


FIG. 8: (Fit 1, red lines); $\pi^0$ photoproduction close to threshold. The $\pi^+ n$ threshold is indicated with an arrow. Experimental analyses: black (gray, empty) data points from Refs. [41] ([42, 43]). Gray band from Ref. [42]. Theory: Blue double dashed dotted lines: MAID 2007 [25], brown dashed lines: Ref. [44]. Dashed dotted lines: ChPT calculation from Ref. [45] (see also the more recent work of Ref. [46]).

TABLE III: Parameters of Fit 1 (low energy $\pi N \to \pi N$ and $\gamma N \to \pi N$). The parentheses indicate weakly correlated parameters.

| | | | | | |
|---|---|---|---|---|---|
| $a_{K\Sigma}$ | $(-3.80)$ | $a_{K\Lambda}$ | $(3.80)$ | $a_{\pi N}$ | 2.65 | $a_{\eta N}$ | 0.49 |

# *Results:* *Phases of the N*(1535) in πN→πN and γN→πN in the present model*

$S_{11}$ & $S_{31}$ ampl. in πN→πN

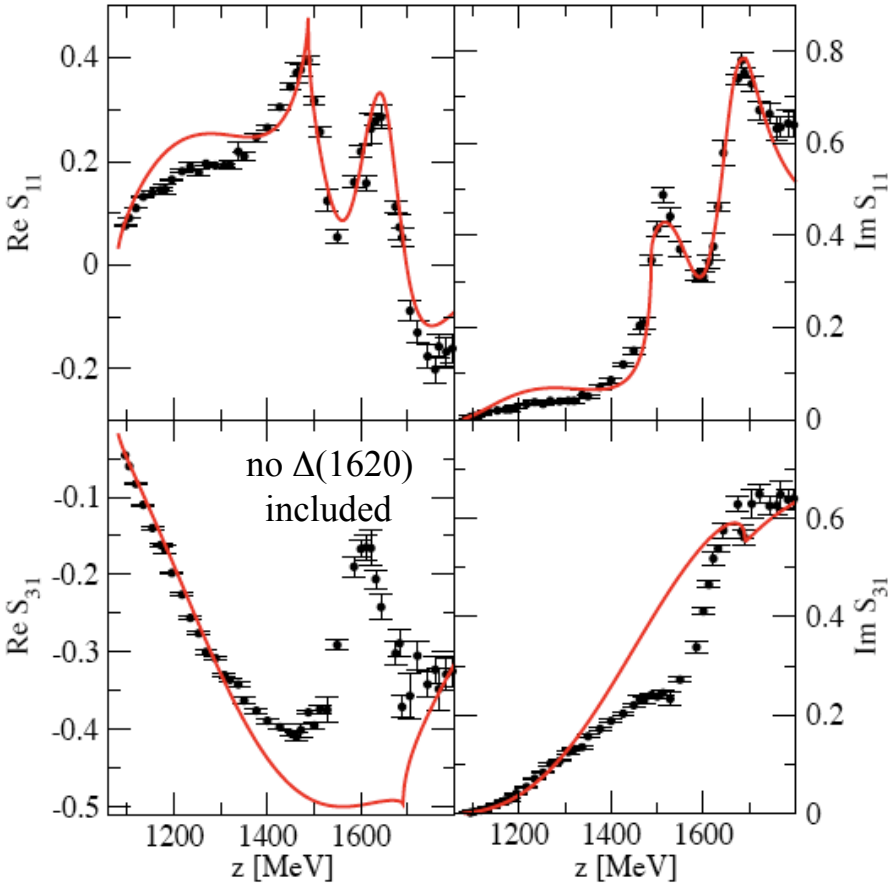


FIG. 11: Data points: SES $\pi N \to \pi N$ partial wave analysis from Ref. [36] [FA07]. Red line: Joint analysis of $\pi N \to \pi N$ and $\gamma N \to \pi N$ (Fit 2).

$E_{0+}$ in γN→πN

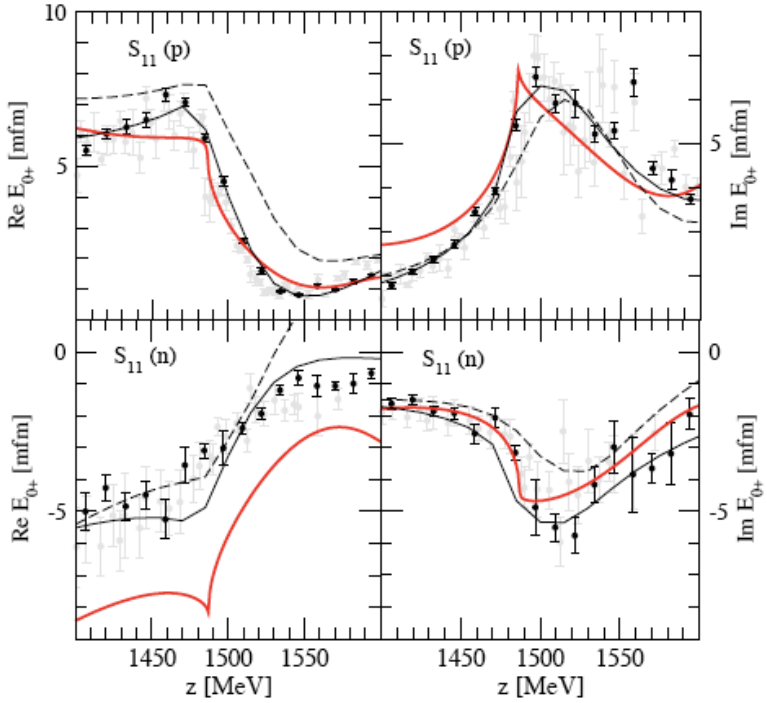


FIG. 13: Detail of Fig. 12 in the $N^*(1535)$ region. Note the form of the cusp at the $\eta N$ threshold is quite different from the $\pi N \to \pi N$ reaction.

important interference effects with the N*(1650)

# *Results:* *πN→πN and γN→πN in the N*(1535) region (parameters of the present model)*

TABLE IV: Parameters of Fit 2 ($\pi N \to \pi N$ and $\gamma N \to \pi N$, entire energy region). Subtraction constants, bare strong and electromagnetic couplings, and bare masses [cf. Eqs. (3, 29)]. The parentheses indicate weakly correlated parameters.

| | | | | | |
|---|---|---|---|---|---|
| $a_{K\Sigma}$ | $-2.04$ | $g_8^{(1)}$ | $0.42$ | $g_8^{(2)}$ | $(2.73)$ |
| $a_{K\Lambda}$ | $3.80$ | $g_{8'}^{(1)}$ | $-0.03$ | $g_{8'}^{(2)}$ | $(1.21)$ |
| $a_{\pi N}$ | $1.29$ | $g_{\overline{10}}^{(1)}$ | $-0.21$ | $g_{\overline{10}}^{(2)}$ | $(0.42)$ |
| $a_{\eta N}$ | $0.93$ | $g_{27}^{(1)}$ | $-0.02$ | $g_{27}^{(2)}$ | $(-0.98)$ |
| | | $g_{\gamma pN^*}^{(1)}$ | $0.73$ | $g_{\gamma pN^*}^{(2)}$ | $(4.52)$ |
| | | $g_{\gamma nN^*}^{(1)}$ | $-0.44$ | $g_{\gamma nN^*}^{(2)}$ | $(-8.17)$ |
| | | $m_{\mathrm{b}\,[\mathrm{MeV}]}^{(1)}$ | $1598$ | $m_{\mathrm{b}\,[\mathrm{MeV}]}^{(2)}$ | $(3800)$ |

# *Pole positions and residues: discontinuity of G*

The hadronic amplitude can be continued analytically into the complex energy ($z=s^{1/2}$)-plane. There are two different Riemann sheets for each channel $\pi N$, $\eta N$, $K\Lambda$, and $K\Sigma$ :

1st sheet: $G^{(1)}(z) = G(z),$

2nd sheet: $G^{(2)}(z) = G(z) + 2\,\dfrac{i\,M\,q_{\rm on}^{>}}{4\pi\,z}$

allows to search for virtual states and hidden poles

discontinuity of G along the right hand cut

M=baryon mass of a given channel

$$q_{\rm on}^{>} = \begin{cases} -q_{\rm on} & \text{if Im } q_{\rm on} < 0 \\ q_{\rm on} & \text{else} \end{cases}$$

Some authors search the poles only on one combination of the sheets:

Inoue et al., PRC65,'02

(does not find virtual states and hidden poles)

Sarkar et al., NPA750,'05

$$\bar{G}_i(z) = \begin{cases} G_i^{(1)}(z) & \text{if Re } z < m_i + M_i \\ G_i^{(2)}(z) & \text{if Re } z \geq m_i + M_i. \end{cases}$$

induced Riemann sheet by G is closest to the physical axis

# *Pole positions and residues: "Gaussian plots"*

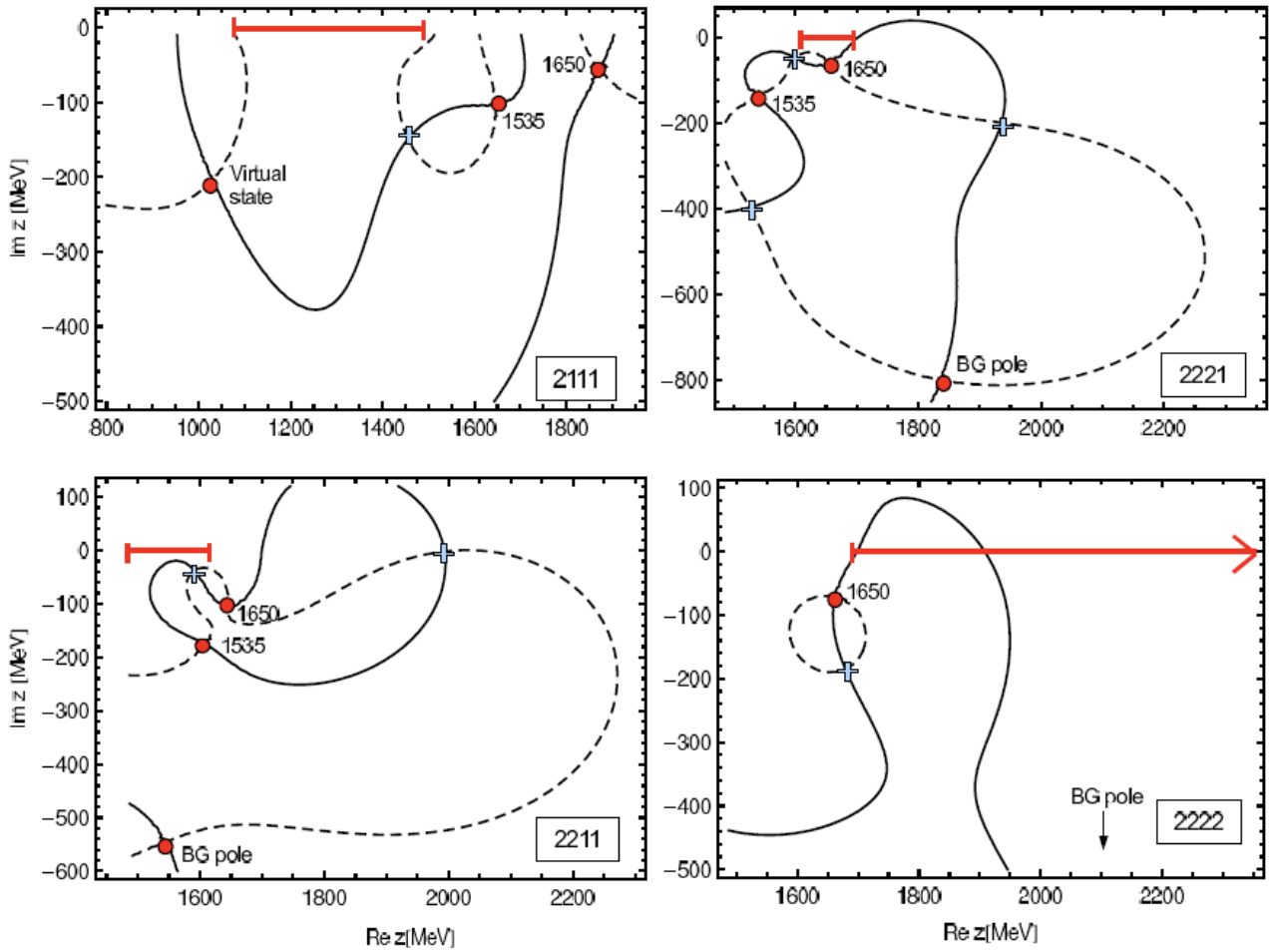


| | Position [MeV] | $g_{\pi^- p}$ |
|---|---|---|
| Sheet 2111 | | |
| VS | $1031 - 203\,i$ | $-0.51 + 1.58\,i$ |
| $N^*(1535)$ | $1647 - 103\,i$ | $-1.55 + 1.40\,i$ |
| $N^*(1650)$ | $1872 - 57\,i$ | $0.91 + 2.64\,i$ |
| Sheet 2211 | | |
| $N^*(1535)$ | $1608 - 175\,i$ | $3.35 + 1.82\,i$ |
| $N^*(1650)$ | $1645 - 105\,i$ | $-1.83 + 1.88\,i$ |
| BG | $1545 - 545\,i$ | $-0.78 + 3.52\,i$ |
| Sheet 2221 | | |
| $N^*(1535)$ | $1538 - 139\,i$ | $1.42 + 0.46\,i$ |
| $N^*(1650)$ | $1655 - 59\,i$ | $-0.89 + 0.48\,i$ |
| BG | $1837 - 800\,i$ | $0.31 + 2.39\,i$ |
| Sheet 2222 | | |
| $N^*(1535)$ | no pole | |
| $N^*(1650)$ | $1662 - 72\,i$ | $-1.03 + 0.12\,i$ |
| BG | $2129 - 1289\,i$ | $0.33 + 2.26\,i$ |

——— Re[T]=0

- - - - Im[T]=0

red line: part of the physical axis directly connected to the respective sheet.

Notation:

$1 \rightarrow G^{(1)}(z)$
$2 \rightarrow G^{(2)}(z)$

e.g.

2111: unphysical wrt πN, physical wrt others

2211: unphysical wrt πN&ηN physical wrt KΛ&KΣ

# *Pole positions and residues: "Gaussian plots"*

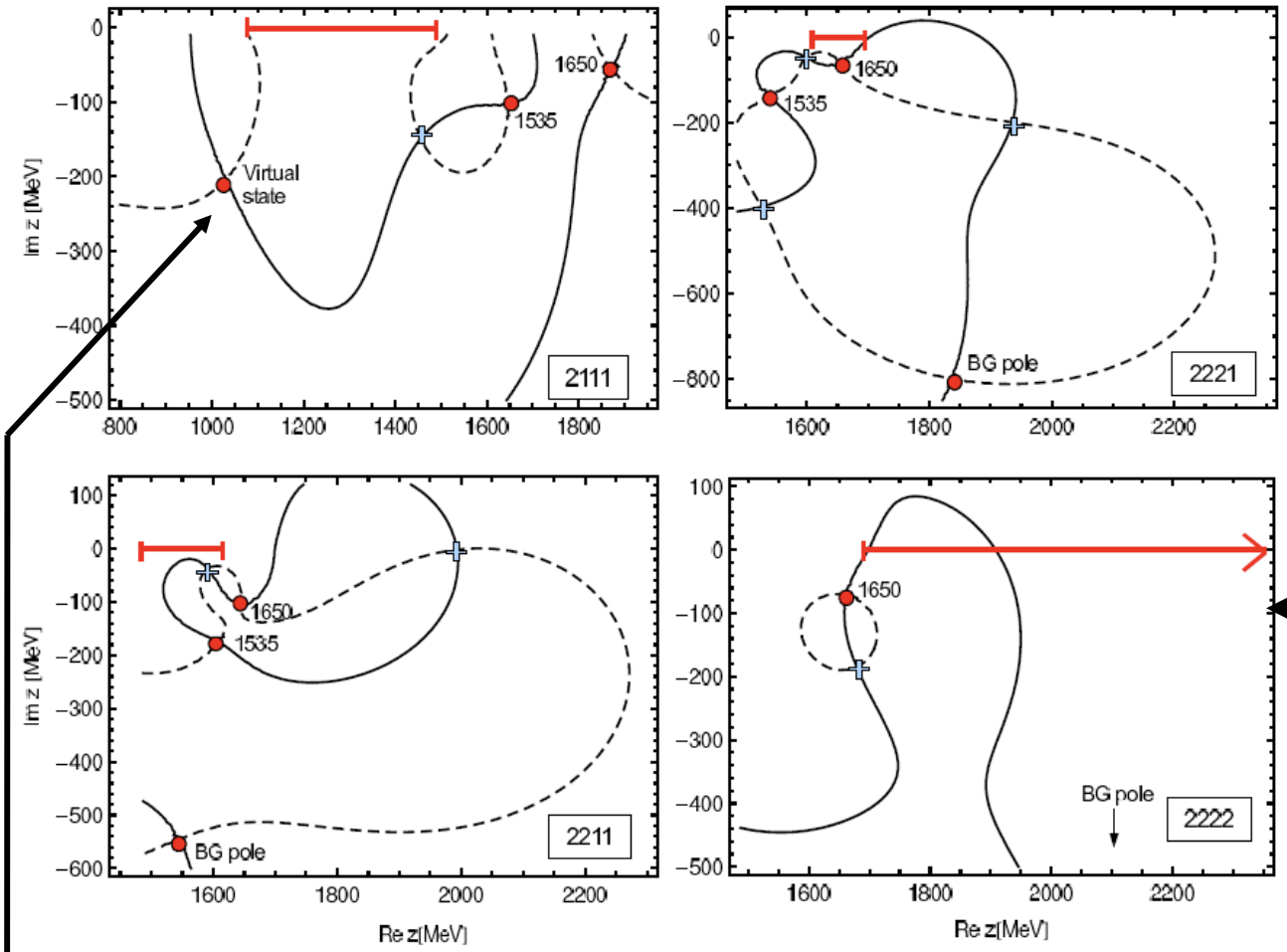


virtual state below πN thres.

model indep. behavior:
sub-thres. resonance with strong coupling [KΣ→ N*(1535)] ⇒ pole is necessarily displaced.

consequenses for calc. trying to describe the data in terms of sub-thres. resonances

# *Pole positions and residues: Shape of the $S_{11}$ ampl.*

Re[$S_{11}$] πN ampl.

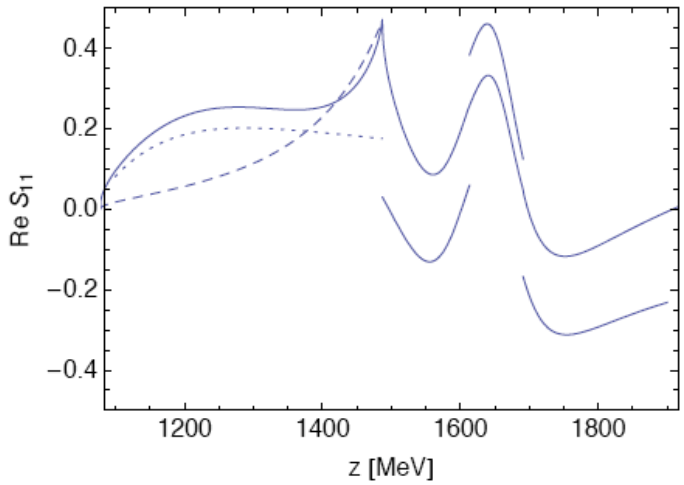


…. virtual state on sheet 2111
---- hidden N*(1535) on sheel 2111

—— $T_{\rm PA}^{(i)} = \sum_j \frac{a_{-1}^j}{z - z_0^j}$ i=2211,2221,2222 ; j=poles

FIG. 15: Pole approximations $T_{\rm PA}^{(i)}$ (piecewise defined lines) of the full solution for Re $S_{11}$. The pieces of the PA are limited by the thresholds of the channels $\pi N$, $\eta N$, $K\Lambda$ and $K\Sigma$.

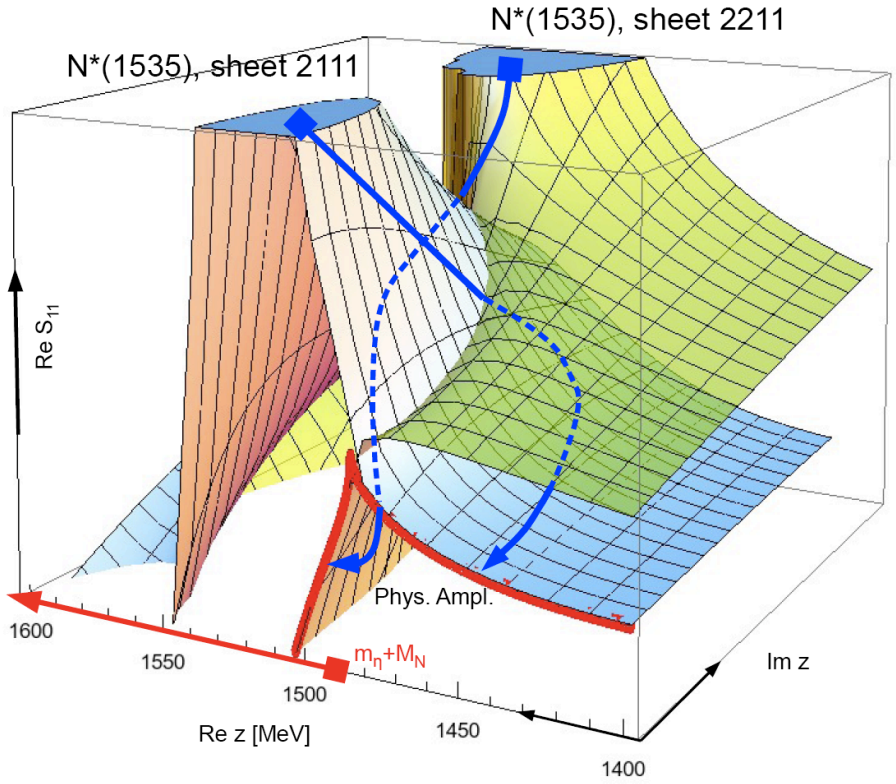

# *Conclusions: phases of N*(1535)*

• The simultaneous study of $\pi N \to \pi N$ and $\gamma N \to \pi N$ in the S partial waves reveals a phase inconsistency of the N*(1535) in the previous description of dynamical generation of this resonance within the U$\chi$PT [Inoue et al., PRC65,'02].

• The origin of this inconsistency has been shown to be largely due to the lack of resonance interference effects between N*(1535) and N*(1650) in the previous model. This has been verified in the present study which extends the previous model by including two genuine 3-quark resonances. One of them becomes N*(1650) but the other one becomes a BG-pole and simulates some of the background processes missing in the model. The N*(1535) is generated dynamically as the (strong) coupling to the strange channels is still dictated by the Weinberg-Tomozawa contact interaction In conjuction with SU(3) structure and the Kaon decay constant of $f_K \approx 113$ MeV.

• A much better fit to the "data" in $\pi N$-$\pi N$ and $\gamma N$-$\pi N$ in the S-partial-wave states is achieved compared to the earlier models. In particular, the currently data do not rule out the scenario of the dynamically generated N*(1535). However, whether or not this scenario is indeed the case, remains to be seen. In this sense, higher partial wave states need to be looked too in particular.

# *Conclusions: analytic structure of the reaction ampl.*

- A detailed study of the analytic structure of the reaction amplitudes has revealed the role of the N*(1535) and N*(1650) poles on different sheets:
  - In particular, the pronounced cusp at the ηN threshold appears as a result of an interplay of the physical and hidden poles on the different Riemann sheets.
  - Poles in different sheets affect the behavior of the reaction amplitude on the physical axis.
  - The N*(1535) on the physical sheet w.r.t. the KΣ channel has disappeared. This has important consequences for calculations which tries to describe reaction processes based on sub-threshold resonances. As the coupling of a sub-threshold resonance to the channel in question increases, its pole position will be necessarily displaced. This behavior is model independent.

- A virtual state (pole below the πN threshold) has been found which is responsible for the sharp rise of the real part of the $S_{11}$ amplitude close to threshold. It may be a forced pole which mocks up the sub-threshold cuts [Arndt]. One should also look in other models/analyses if this pole is present.

# *Motivation: $\sigma_p$ & $\sigma_n$ in η photoproduction:*

Excess of η in quasi-free γn → ηn :

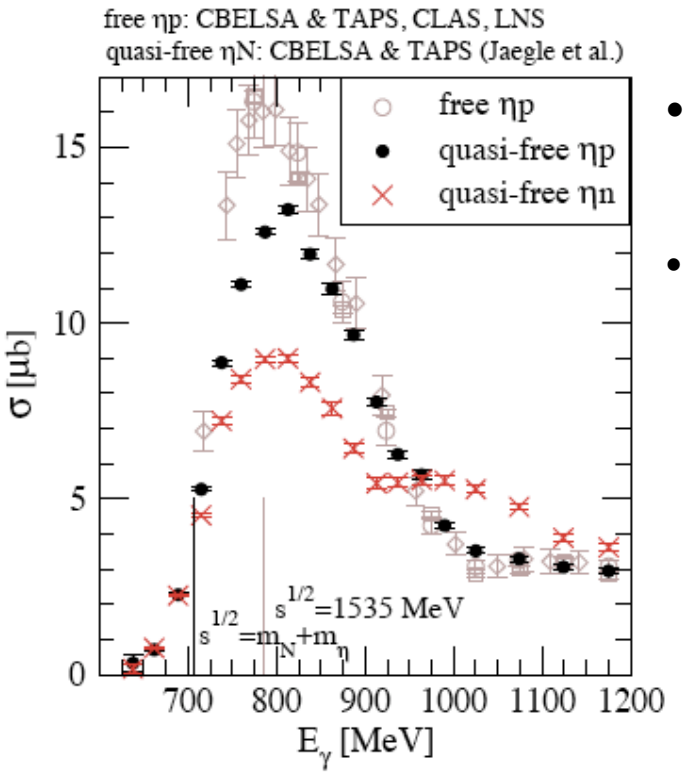


- Excess of η on n found by GRAAL [Kuznetsov et al., PLB647,'07]
  confirmed by CBELSA & TAPS [Jaegle et al., PRL100,'09]
  and LNS [Miyahara et al., PTPS168,'07]
- Vivid discussion: workshop on *Narrow Nuclear Resonances*, Edinburgh, June'09, [http://2009physicsevents.org/pages/speakers.hmtl]
  - non-strange pentaquark [Diakonov et al., ZPA359,'97, Polyakov et al., EPJA18, '03,…]
  - $S_{11}(1650)/P_{11}(1710)$ interference [Shklyar et at., PLB650,'09]
  - interference of various partial waves [Choi et al., PLB363'06; Shyan et al., arXiv:0808.0632]
  - $D_{15}(1675)$ [ηMAID, NPA700'02] or $P_{11}$ [Fix et al., EPJA32'07]
  - ≈ 80% of $\sigma_p$ is S-wave; how about $\sigma_n$?
    P-wave? polarization data. [Kuznetsov, Polyakov et al., APPolonB39 …,'08]
    S-wave dominance? [Anisovich et al., EPJA41,'09; Miyahara et al., PTPS168,'07]

# *Motivation: $\sigma_p$ & $\sigma_n$ in η photoproduction:*

Excess of η in quasi-free γn → ηn :

[Kuznetsov &Polyakov, JETP88,'08]

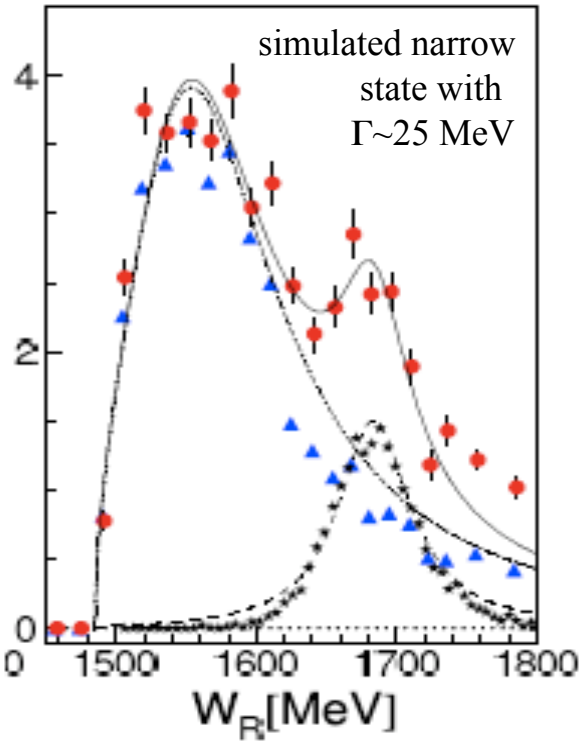


Fig. 2. $M(\eta n)$ spectrum from CBELSA/TAPS [12] (filled circle) in comparison with $M(\eta p)$ spectrum (filled triangles) Stars show the simulated signal of a narrow state.

- Excess of η on n found by GRAAL [Kuznetsov et al., PLB647,'07]
  confirmed by CBELSA & TAPS [Jaegle et al., PRL100,'09]
  and LNS [Miyahara et al., PTPS168,'07]
- Vivid discussion: workshop on *Narrow Nuclear Resonances*, Edinburgh, June'09, [http://2009physicsevents.org/pages/speakers.hmtl]
  - non-strange pentaquark [Diakonov et al., ZPA359,'97, Polyakov et al., EPJA18, '03,…]
  - $S_{11}(1650)/P_{11}(1710)$ interference [Shklyar et at., PLB650,'09]
  - interference of various partial waves [Choi et al., PLB363'06; Shyan et al., arXiv:0808.0632]
  - $D_{15}(1675)$ [ηMAID, NPA700'02] or $P_{11}$ [Fix et al., EPJA32'07]
  - ≈ 80% of $\sigma_p$ is S-wave; how about $\sigma_n$?
    P-wave? polarization data. [Kuznetsov, Polyakov et al., APPolonB39 …,'08]

    S-wave dominance? [Anisovich et al., EPJA41,'09; Miyahara et al., PTPS168,'07]

# *Results:* *η photoproduction on proton and neutron*

**free**

solid : γp → ηp
dotted: γn → ηn

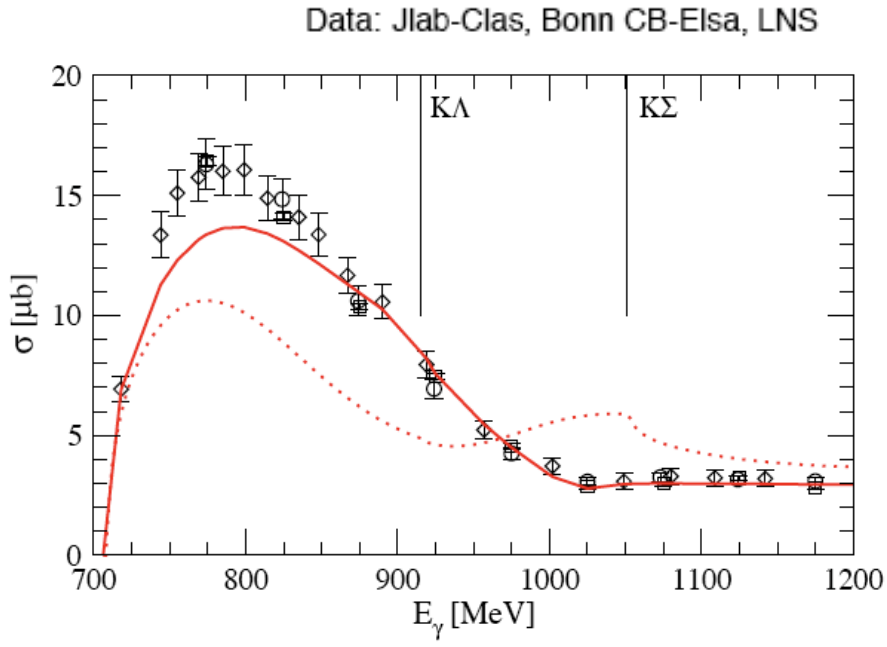


**quasi-free**

solid : γp → ηp
dotted: γn → ηn

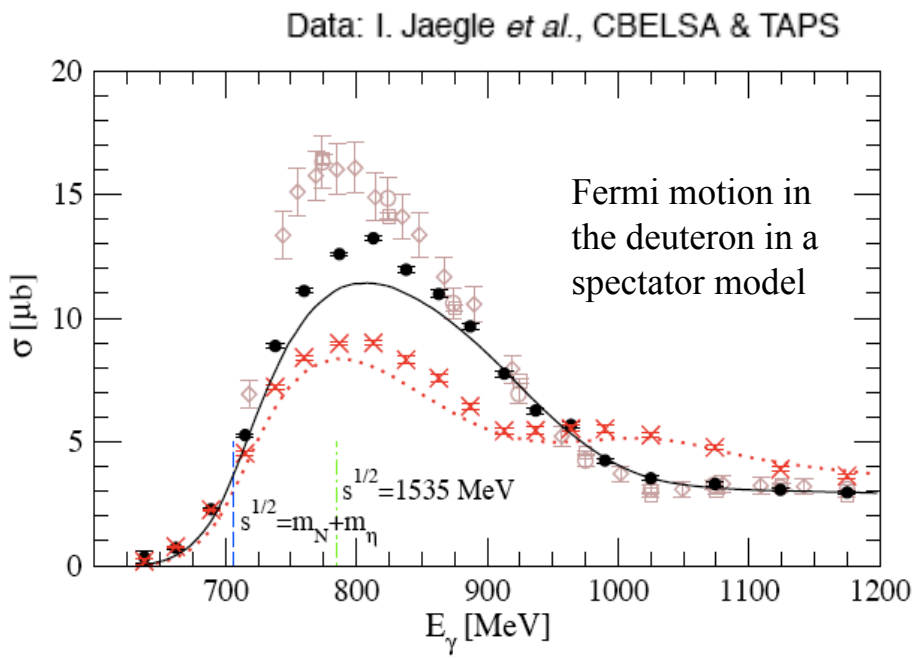


intermediate state in the photon loops:

neutron: $\pi^-p$, $\pi^0n$, $\eta n$, $K^0\Lambda$, $K^+\Sigma^-$, $K^0\Sigma^0$

proton : $\pi^0p$, $\pi^+n$, $\eta n$, $K^+\Lambda$, $K^+\Sigma^0$, $K^0\Sigma^+$

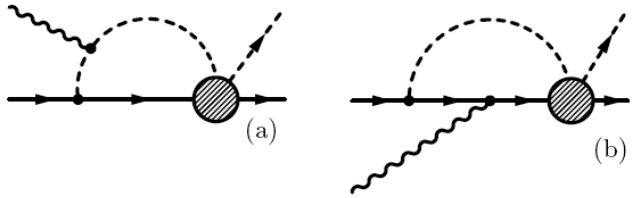

# *Results : cross section ratio $\sigma_n/\sigma_p$*

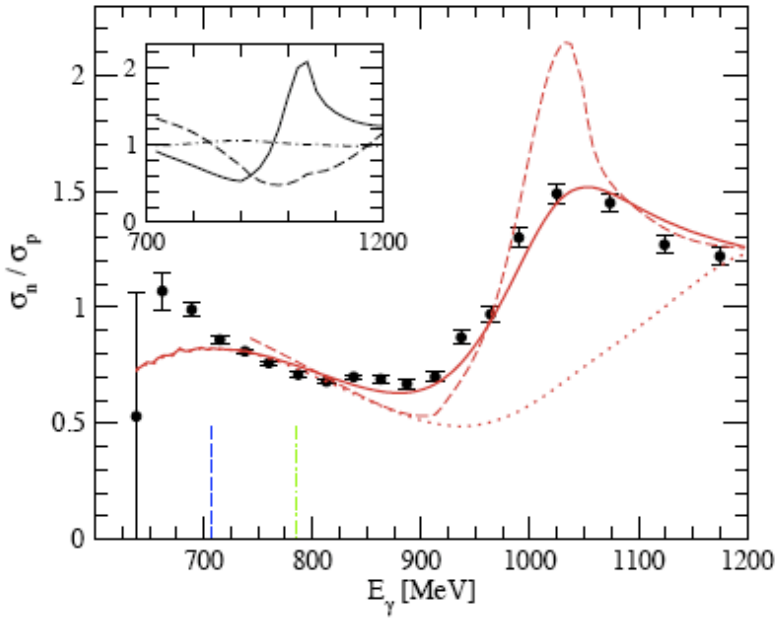


Data: I. Jaegle *et al.*, CBELSA & TAPS

- Peak in $\sigma_n/\sigma_p$ :
  direct consequence of the Weinberg-Tomozawa interaction with the strong couplings to KΛ and KΣ channels given by SU(3) (and $f_K \cong 113$ MeV).
- Simple and quantitative explanation.

solid : full result (with Fermi motion)
dashed: no Fermi motion
dotted: no $K^+\Lambda$ intermediate state
inset (dash-dotted): only πN intermediate state

# *Test of η photoproduction*

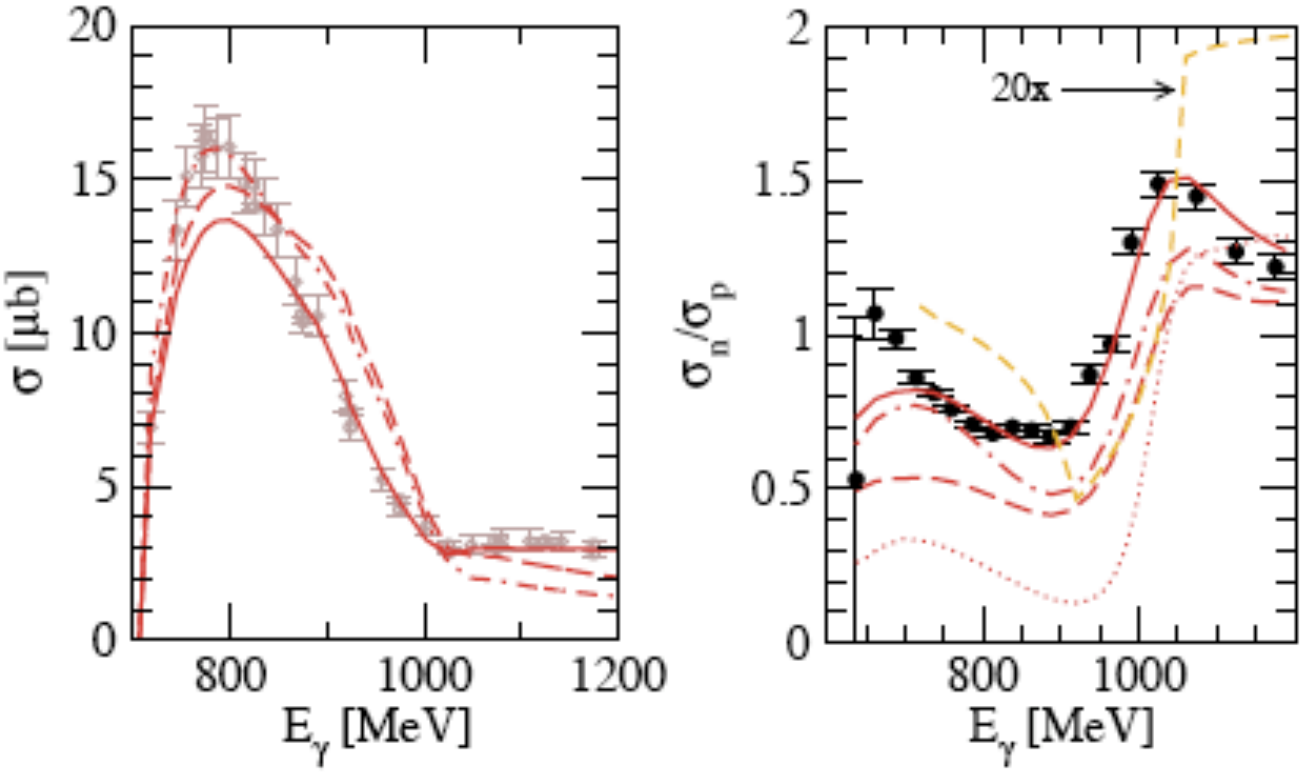


Solid: present results
Dashed: incl. higher order baryon terms
Dash-dotted: incl. ππN
Dotted : no bare resonances
Dashed: only the WT term in the FSI (no Fermi).

# *Hadronic transitions:* $\pi N \to \pi N,\ \eta N,\ K\Lambda,\ K\Sigma$

$\pi N \to \pi N$

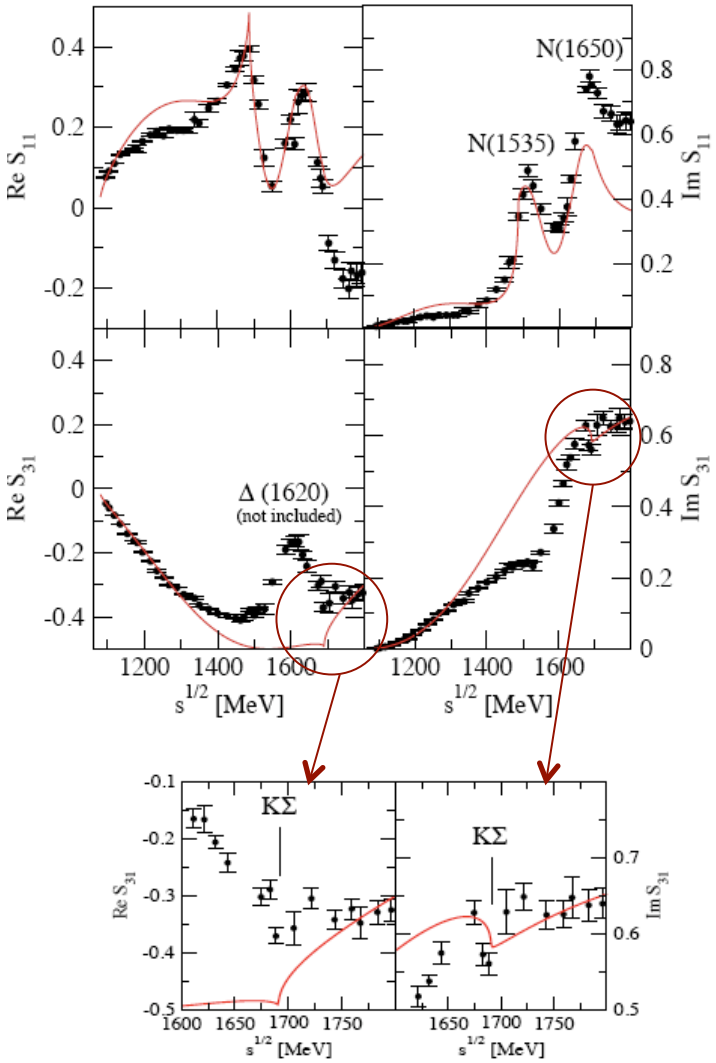


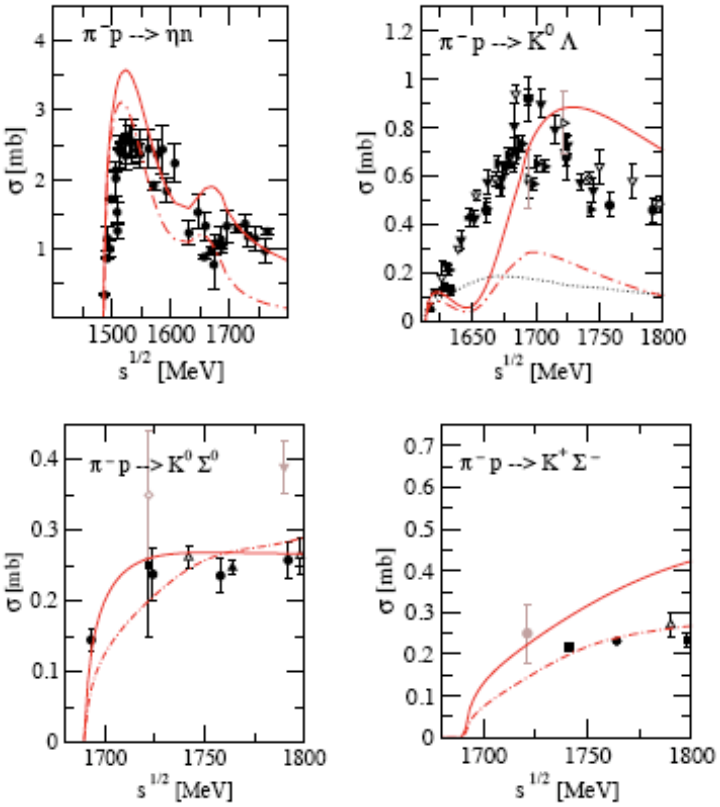

# *Photoproduction:* $\gamma N \rightarrow \pi N, K\Lambda, K\Sigma$

$\gamma N \rightarrow \pi N$

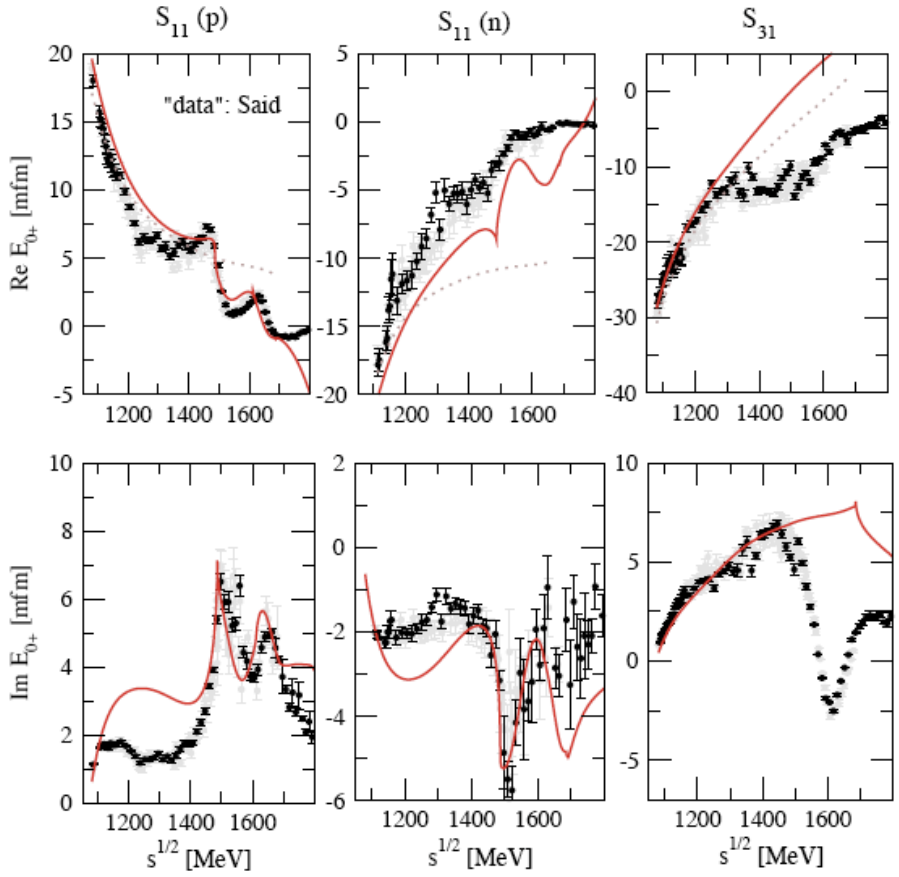


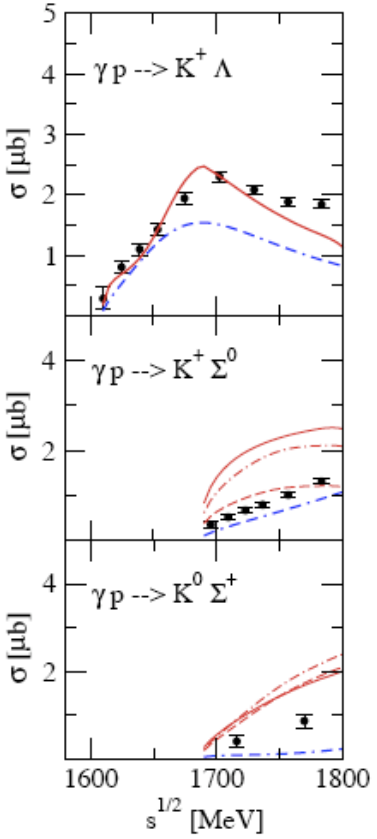

# *Prediction of $\sigma_n/\sigma_p$ in $\gamma N \to K\Lambda$*

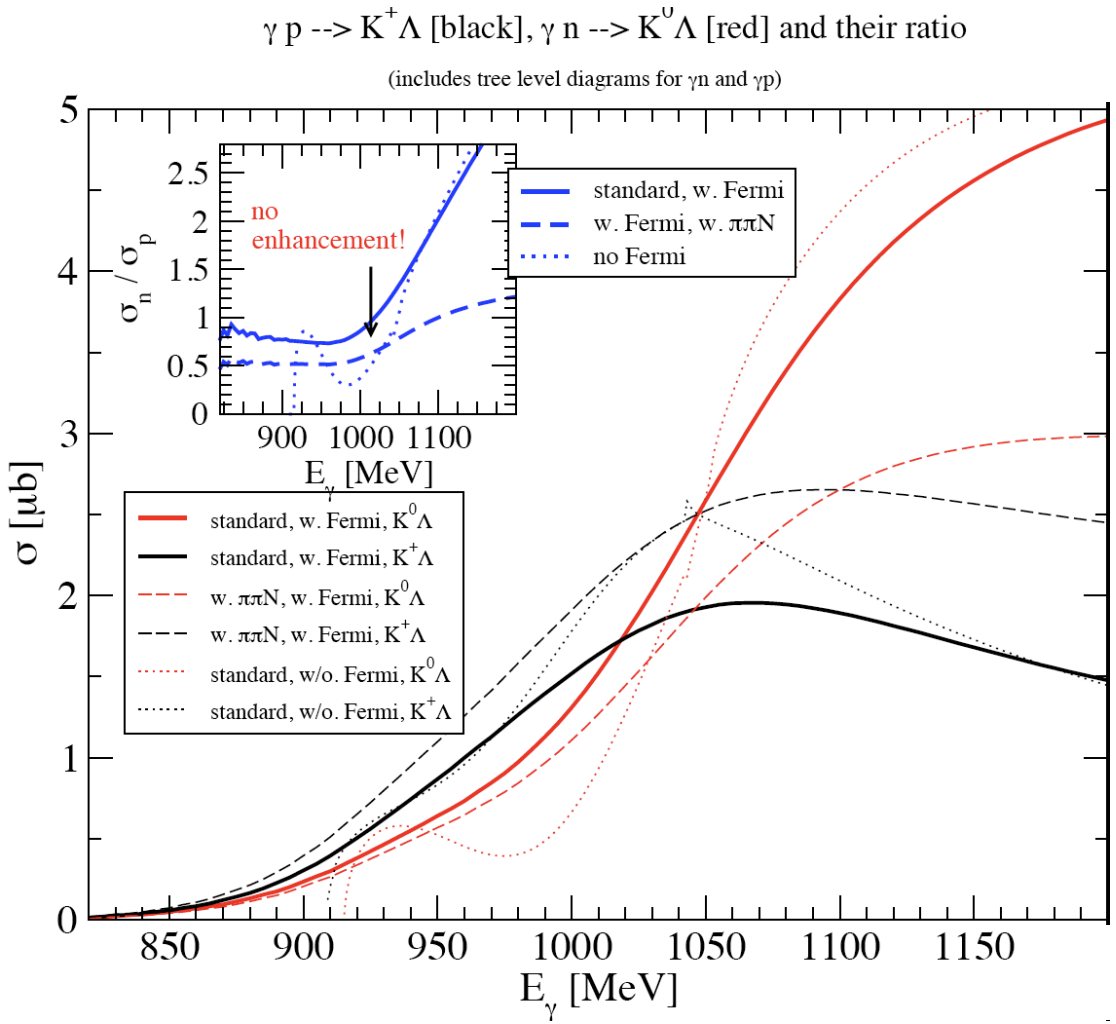


$\gamma N \to K\Lambda$
might be able to test the coupled channel effect
vrs
pentaquark

# *Conclusions*

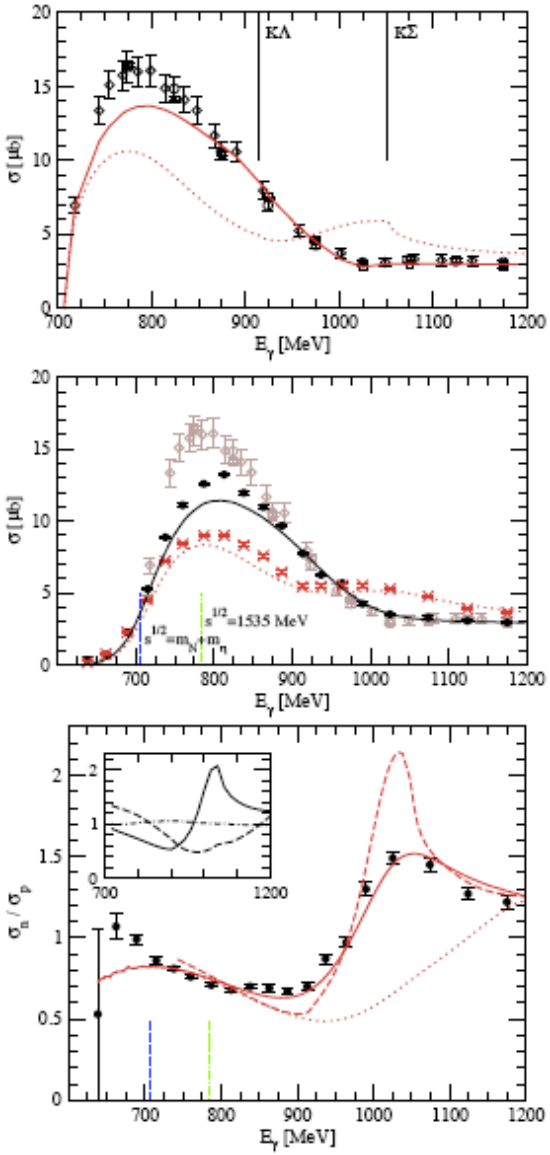


- Global fit (18 params.) of 11 photoproduction and 8 hadronic independent reaction data sets, spanning 700 MeV in energy and involving πN, ηN, KΛ, KΣ final states.
- $\gamma n \rightarrow \eta n$: intermediate KΛ, KΣ loops with photon couplings lead to KΣ threshold enhancement (peak in $\sigma_n/\sigma_p$).
- Consequence of underlying hadron dynamics: Weinberg-Tomozawa term from chiral Lagrangian induces strong channel coupling through its SU(3) structure. [N*(1535) is here dynamically generated]
- Peak in sn/sp is a stable feature, resistant to various tests like
  - removal of genuine resonance states.
  - inclusion of higher-order baryon pole terms.
  - inclusion of ppN channel.
- Higher partial-waves need to be checked.
  (maybe in meson-exchange dynamical models)
- Other explanations (narrow resonance) are not ruled out.

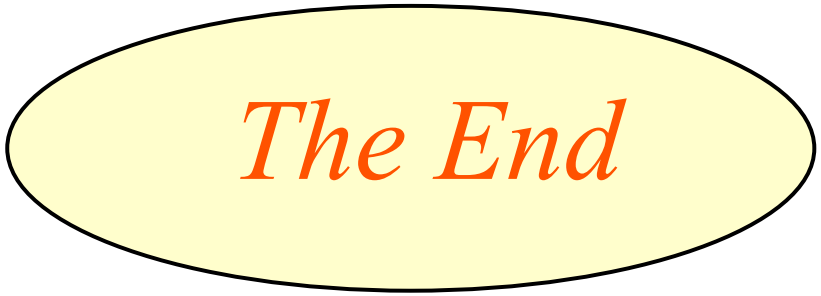
The End